Rapid magma ascent recorded by water diffusion profiles in mantle olivine

Sylvie Demouchy, Steven D. Jacobsen, Fabrice Gaillard, Charles R. Stern

GSA Data Repository item 2006084

Rapid magma ascent recorded by water diffusion profiles in mantle olivine

S. Demouchy, S. D. Jacobsen, F. Gaillard and C. R. Stern

Methods and samples

Chemical composition

After infrared measurements, minerals were analysed for chemical composition using a Cameca SX50 electron microprobe (15 keV, 15nA, point beam and 20 s counting time). Multi-component profiles were measured but did not reveal chemical zoning between core and rim in the olivine grains. Representative chemical analyses are provided in the Table DR1.

Transmission electron microscopy (TEM)

TEM observations on one of the olivine grains (PA-3) revealed no water-rich precipitates or hydrous defect layers, e.g., humite lamellae *(Miller et al., 1987)*, no high density of dislocations, and no melt pockets revealing early partial melting phenomenon *(Raterron et al., 1997)*.

Table DR1. Chemical composition of each mineral phase in Pali-Aike peridotite xenoliths.

Xenolith sample	LS 33	LS 33	Palix-1	Palix-1	Palix-1	Palix-1	Palix-1
Mineral	olivine	olivine	Olivine PA-1	Olivine PA-11	opx	diop	garnet
Element (wt.%)							
SiO_2	41.30	41.49	40.91	40.77	55.22	52.36	42.25
TiO_2	BDL	BDL	BDL	BDL	0.07	0.45	0.16
$Al2O_3$	0.05	0.06	0.04	0.03	3.72	5.26	22.73
$Cr2O_3$	0.01	0.03	0.02	0.06	0.52	1.33	1.68
FeO	9.22	9.06	9.52	9.72	6.12	3.13	7.55
MnO	0.09	0.08	0.11	0.12	0.09	0.06	0.29
MgO	49.66	50.03	49.70	49.82	33.56	15.86	20.88
CaO	0.11	0.09	0.06	0.05	0.74	19.02	4.99
Na_2O	BDL	BDL	0.00	0.02	0.12	1.74	0.02
NiO	0.30	0.44	0.38	0.49	0.14	0.03	0.03
Sum	100.74	101.28	100.75	101.07	100.20	99.24	100.57
H_2O (wt. ppm)*					310 ± 105	416 ± 150	<1
H_2O (wt. ppm)†	28 ± 10	32 ± 10	56 ± 18	35 ± 10			
Mg#	90.57	90.78	91.08	91.08			
Ens#					89.43	50.70	
Fs#					1.42	43.69	
Wo#					9.15	5.61	

Note: "BDL" below detection limit,
"opx": orthopyroxene,
" diop": diopside.
* water contents are given using the calibration of Paterson (Paterson, 1982) from unpolarized FTIR spectra for pyroxenes
† are water contents for olivine only, corrected following the recommendations of Bell et al. (2003).

FTIR measurement

FTIR spectroscopy was performed with a Bruker^{TM} IFS 120 HR high-resolution FTIR spectrometer coupled with a Bruker^{TM} IR microscope. More than 30 olivine grains and 15 pyroxenes and garnet were studied. All of them were studied with unpolarized FTIR spectroscopy and 2 large olivines were selected for polarised FTIR and diffusion analysis. Two hundred scans were accumulated for each spectrum at a resolution of 1 cm^{-1}. The beam was focused in the sample using a 1.5 mm aperture, which generated a spot size of 100 μm in the focal plane. After a background baseline correction, the water content was quantified in each mineral with the calibration of Paterson (1987)

$$C_{OH} = \frac{Xi}{150\,\gamma} \int \frac{K(\bar{v})}{(3780 - \bar{v})}\, d\bar{v} \tag{1}$$

where $k\,(v)$ is the absorption coefficient at wavenumber v, Xi is the density factor (for olivine equal to 2695 wt ppm H_2O using the calibration of Paterson (1987) and equal to 3.5×2695 wt ppm H_2O following the correction of Bell et al. (2003), for diopside: 2769 wt ppm H_2O, and for orthopyroxene: 2727 wt ppm H_2O (Bolfan-Casanova et al., 2000), γ is the orientation factor (equal to 1/3 for unpolarized spectra and 1 for polarized spectra with E parallel to the O-H bond direction). For polarized FTIR spectra of olivine, the calibration of Bell and co-workers (Bell et al. 2003) was used

$$C_{OH} = \frac{1}{I}\left[\left(\int k(v)\,dv\right)_{[100]} + \left(\int k(v)\,dv\right)_{[010]} + \left(\int k(v)\,dv\right)_{[001]}\right] \tag{2}$$

with $\qquad\qquad I = I_{//}\gamma \tag{3}$

where $k(v)_{[xyz]}$ is the absorption coefficient at wavenumber v with E (electric vector) parallel to [100], [010] or [001], $I_{//}$ is the integral extinction coefficient (here assumed (Bell et al., 2003) to be 5.32 cm^{-2} per wt ppm H_2O), γ is the orientation factor equal to 1 for polarized spectra with E parallel to the O-H bond direction. For both calibrations, integration was performed between 3650 and 3050 cm^{-1}. To form a profile, spectra were collected at a spacing of 50 µm near the edges of the sample and 100 µm near the center of the sample (Fig. DR1).

Table DR2. Water contents of the minerals in Pali-Aike garnet-lherzolite xenolith.

Sample	(1) Water content wt ppm H_2O	(2) Water content wt ppm H_2O	(3) Water content wt ppm H_2O
FTIR Calibration	Paterson (1982)	Value in (1) corrected by a factor 3.5 as recommended by Bell et al (2003)	Bell et al (2003) For olivine only
Diopside	416 ± 150	-	-
Enstatite	310 ± 105	-	-
Olivine PA-1	16 ± 5	56 ± 18	-
Olivine PA-3	-	-	24 ± 2
Olivine PA-7 observed	15 ± 4	53 ± 14	45 ± 4
Olivine PA-7, estimated prior to dehydration	~ 104		~ 312
Uppermost mantle* beneath Patagonia prior to dehydration,	~ 170		

Note: (1) water content using the calibration of Paterson (1987) for unpolarized FTIR spectra. (2) values given in (1) corrected for olivine only using the recommendations of Bell et al. (2003) by a factor of 3.5. (3) water content applying strictly the recent calibration of Bell et al. (2003) for polarized FTIR spectra in olivine, comparison with unpolarized data give a factor 3 for olivine. Values reported for olivine were measured in the core of each sample. (*) Uppermost mantle composed of 0.66 % olivine+ 0.27 % orthopyroxene + 0.03 % clinopyroxene + 0.04 % garnet, (see also Bell and Rossman, 1992; Ingrin and Skogby, 2000).
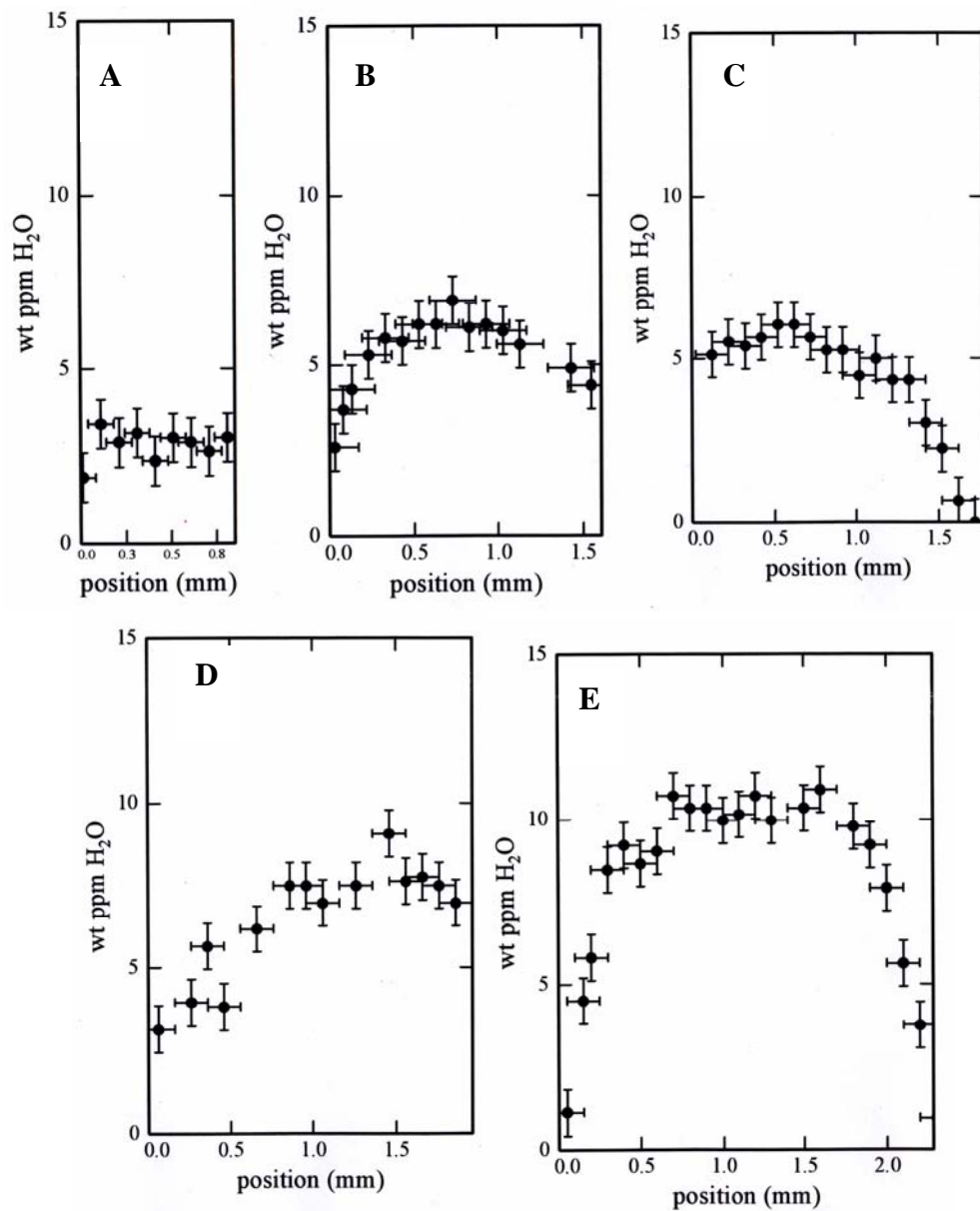
Fig. DR1. Five profiles of unpolarized infrared spectra across different unoriented olivine crystals: (A) olivine PA-16, 0.86 mm, (B) olivine PA-14, 1.61 mm, (C) olivine PA-18, 1.77 mm, (D) olivine PA-2, 1.96 mm, (E) olivine PA-11, 2.26 mm. They show hydroxyl-depleted rims. The water contents were obtained using the calibration of Paterson (1982). Values on Y axis may be time by a factor 3.5 to have an estimate following the Bell et al. (2003) calibration.

Diffusion analysis

In order to calculate theoretical diffusion profiles, the initial water contents were estimated in the following manner. The temperature of the host basalt is estimated to be between 1200 and 1290°C. Assuming equilibrium in the mantle source region, orthopyroxene and olivine must reflect the same water fugacity (Kohlstedt et al., 1996; Mierdel and Keppler, 2004; Rauch and Keppler, 2002). Thus, the water content within orthopyroxene of ~ 310 wt ppm H_2O corresponds to a water fugacity of ~1.5 GPa, which suggests a water content of ~ 312 wt ppm H_2O within olivine, using the results from Kohlstedt et al. (1996) and corrected using the recommendations (correction factor) of Bell et al. (2003). When using polarized infrared spectra to determine total water contents in a grain of olivine, we must allow for the anisotropic distribution in water. From the spectra of experimentally water-saturated olivine presented by Bell et al. (2003), ~ 115 wt ppm H_2O would be measured with E parallel to [100] (37% of the total water content of ~312 wt ppm H_2O), 62 wt ppm H_2O (20%) parallel to [010], and ~134 ppm H_2O (43%) parallel to [001]. These values were used to estimate the water content for E parallel to [010] from the concentrations observed for E parallel to the [100] and [001] axes in olivine PA-7. We approximate the system by considering the

xenolithic olivine crystal as a parallelepiped with anisotropic diffusion. A better model would use anisotropic diffusion in an ellipsoid; this difference explains the difference between the observed and calculated profiles. In such a system, we assume that hydrogen diffusion in grain boundaries is significantly faster than hydrogen lattice diffusion (no differences were observed between water content in olivines in the middle or in the borders of the studied lherzolite xenoliths). Therefore the observed profiles reflect the hydrogen lattice diffusion in olivine. The water content (hydrogen as the diffusing specie) in three-dimensions can then be described by the function $v(x,y,z)$ (Crank, 1956), where the width of the grain in the x direction is 2a, in the y direction 2b and in the z direction 2c:

$$
\begin{aligned}
v(x,y,z) = \ & \frac{64}{\pi^3} \sum_{l=0}^{\infty} \sum_{m=0}^{\infty} \sum_{n=0}^{\infty} \frac{(-1)^{l+m+n}}{(2l+1)(2m+1)(2n+1)} \ \times \\
& \cos\frac{(2l+1)\pi x}{2a} \ \cos\frac{(2m+1)\pi y}{2b} \ \cos\frac{(2n+1)\pi z}{2c} \ \times \\
& \left[\exp-\frac{\pi^2 t}{4}\left\{ \frac{D_x\,(2l+1)^2}{a^2} + \frac{D_y\,(2m+1)^2}{b^2} + \frac{D_z\,(2n+1)^2}{c^2} \right\} \right] + Ci \quad (4)
\end{aligned}
$$

Here $v(x,y,z)$ is the water concentration at point (x,y,z), t is time, C_i is the initial hydroxyl content, $D_{(x, y, z)}$ is the chemical diffusivity for the mobile species parallel to [100], [010] and [001], respectively. For PA-7 crystal, 2a=2.2mm, 2b=1.7 mm and 2c=1.7mm, $D_x = D_y = 2.4 \times 10^{-12}$ m^2/s and $D_z = 5.2 \times 10^{-11}$ m^2/s at 1245°C, $D_x = D_y = 1.6 \times 10^{-12}$ m^2/s and $D_z = 2.8 \times 10^{-11}$ m^2/s at 1200°C ; and $D_x = D_y = 3.5 \times 10^{-12}$ m^2/s and $D_z = 9.3 \times 10^{-11}$ m^2/s at 1290°C for hydrogen diffusion in iron-bearing olivine limited by metal vacancy diffusion (Demouchy, 2004; Demouchy and Mackwell, 2003; Kohlstedt and Mackwell, 1998, 1999).

References:

Bell, D., Rossman, G., Maldener, J., Endisch, D., and Rauch, F., 2003, Hydroxide in olivine: a quantitative determination of the absolute amount and calibration of the IR spectrum: J. Geophys. Res., v. 108, p. on line.

Bolfan-Casanova, N., Keppler, H., and Rubie, D., 2000, Water partitioning between nominally anhydrous minerals in the MgO-SiO_2-H_2O system up to 24 GPa: Implications for the distribution of water in the Earth's mantle.: Earth Planet. Sci. Lett., v. 182, p. 209-221.

Crank, J., 1956, The mathematics of diffusion: Oxford.

Demouchy, S., and Mackwell, S.J., 2003, Water diffusion in synthetic iron-free forsterite: Phys. Chem. Minerals, v. 30, p. 486-494.

Demouchy, S., 2004, Water in the Earth's interior: Thermodynamics and kinetics of hydrogen incorporation in olivine and wadsleyite, [Ph.D Thesis]: Bayerisches Geoinstitut, Bayreuth Universitaet, 165p.

Kohlstedt, D.L., Keppler, H., and Rubie, D.C., 1996, Solubility of water in the α, β and γ phases of $(Mg,Fe)_2SiO_4$: Contrib. Mineral. Petrol., v. 123, p. 345-357.

Kohlstedt, D.L., and Mackwell, S.J., 1998, Diffusion of hydrogen and intrinsic point defects in olivine: Z. Phys. Chem., v. 207, p. 147-162.

—, 1999, Solubility and diffusion of "water" in silicate minerals, *in* K. Wright, and R. Catlow. (Eds.), eds., Microscopic Properties and Processes in Minerals: Dordrecht, Kluwer Academic Publishers, p. 539-559.

Mackwell, S.J., and Kohlstedt, D.L., 1990, Diffusion of hydrogen in olivine: Implications for water in the mantle: J. Geophys. Res., v. 95, p. 5079-5088.

Mierdel, K., and Keppler, H., 2004, The temperature dependence of water solubility in enstatite: Contrib. Mineral. Petrol., v. 148, p. 305-311.

Miller, G.H., Rossman, G.R., and Harlow, G.E., 1987, The Natural Occurence of Hydroxide in Olivine: Phys. Chem. Minerals, v. 14, p. 461-472.

Paterson, M., 1982, The determination of hydroxyl by infrared absorption in quartz, silicate glasses and similar materials.: Bull. Minéral., v. 105, p. 20-29.

Raterron, P., Bussod, G.Y., Doukhan, J.C., and Doukhan, N., 1997, Early partial melting in the upper

mantle: an A.E.M. study of a lherzolite experimentally annealed at hypersolidus conditions:

Tectonophysics, v. 279, p. 79-91.

Rauch, M., and Keppler, H., 2002, Water solubility in orthopyroxene: Contrib. Mineral. Petrol., v. 143,

p. 525-536.